Structure Elucidation

DOI: 10.1002/anie.201005226

Elansolid A, a Unique Macrolide Antibiotic from *Chitinophaga sancti* Isolated as Two Stable Atropisomers**

Heinrich Steinmetz, Klaus Gerth, Rolf Jansen, Nadin Schläger, Richard Dehn, Silke Reinecke, Andreas Kirschning, and Rolf Müller**

In memory of Jürgen Wehland

Bacterial species of the genera *Flexibacter* and *Chitinophaga* are known to produce biologically active peptides of relevance to anti-infective research because of their interesting mechanisms of action.[1] For instance, the formadicins, monocyclic β-lactam antibiotics from *Flexibacter alginoliquefaciens*, act selectively against pseudomonads and have proven to be hydrolysis-resistant against various types of β-lactamases.[2] The anti-MRSA[3] dipeptides TAN-1057A–D isolated from *Flexibacter* sp.[4] were shown to inhibit peptide elongation during the bacterial translation.[5]

Early work on *Flexibacter* strains by Steinmetz, Gerth, and Höfle resulted in the isolation of a group of novel metabolites named elansolids. The planar structure of the major component was elucidated by spectroscopic methods, degradation by cross-methathesis with ethylene, and biosynthetic reasoning as elansolid A1 (**1**).[6] Later, in the course of our biological screening of extracts from non-myxobacterial gliding bacteria we re-investigated in depth the family of elansolids produced by *Flexibacter sancti*, a species recently reclassified as *Chitinophaga sancti* (comb. nov.).[7] The elansolids are the first polyketide-derived macrolides from the genus *Chitinophaga*.[8]

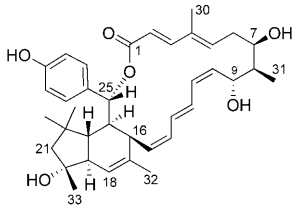

1 and **1***

The basic structure of the elansolids is illustrated with variant A1 (**1**). The HR-ESI mass spectrum of the molecular ion cluster $[M+H]^+$ combined with the ^{13}C and ^{1}H NMR data in $[D_6]$DMSO (Table S1 in the Supporting Information) indicate the elemental composition $C_{37}H_{48}O_6$. The ^{13}C NMR spectrum shows signals for all carbon atoms, and the HMQC spectrum provides the correlations to their directly bound protons, leaving four exchangeable protons.

The structural units derived from $^{1}H,^{1}H$ coupling were interconnected utilizing relevant correlations in the HMBC spectrum as shown in Figure 1. Thus, the largest unit A is linked with the double bond of unit B. Following the HMBC correlations of the carboxy C1 atom ($\delta_C = 165.7$ ppm) with 3-H and 25-H, the carboxy group is used to close a macrolactone ring. Its presence is also supported by the diagnostic downfield shift of the oxymethine 25-H signal appearing at $\delta_H = 5.93$ ppm, which is enhanced by the aromatic residue C

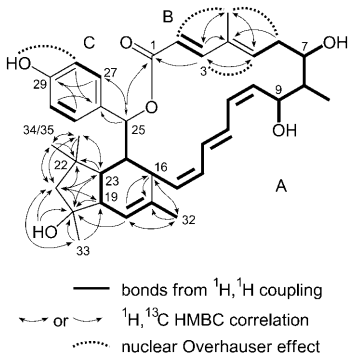

Figure 1. Elansolid A1/A2 (1/1*) and selected correlations from the 2D NMR spectra of 1.

[*] H. Steinmetz, Dr. K. Gerth, Dr. R. Jansen, S. Reinecke, Prof. Dr. R. Müller
Mikrobielle Wirkstoffe, Helmholtz Zentrum für Infektionsforschung
Inhoffenstrasse 7, 38124 Braunschweig (Germany)
Fax: (+49) 531-6181-9499
E-mail: rom@helmholtz-hzi.de
Prof. Dr. R. Müller
Helmholtz Institut für Pharmazeutische Forschung des Saarlandes
Universität des Saarlandes
Postfach 151150, 66041 Saarbrücken (Germany)
N. Schläger, Dr. R. Dehn, Prof. Dr. A. Kirschning
Institut für Organische Chemie und Biomolekulares
Wirkstoffzentrum (BMWZ), Leibniz Universität Hannover
Schneiderberg 1B, 30167 Hannover (Germany)
Fax: (+49) 511-762-3011
E-mail: andreas.kirschning@oci.uni-hannover.de

[**] R.D. thanks the Fonds der chemischen Industrie for a scholarship. We thank W. Kessler and his colleagues for fermentations, F. Sasse for the determination of the cytotoxicity, and C. Kakoschke, B. Jaschok-Kentner, and E. Hofer for expert assistance with the NMR experiments.

Supporting information for this article (tables of NMR data, a table comparing the biological activity of elansolid A1 (**1**) and A2 (**1***), tables comparing the observed and calculated ROESY data and vicinal coupling constants, and a full description of experimental details and chemical data of all compounds) is available on the WWW under http://dx.doi.org/10.1002/anie.201005226.

appended to C25. The *p*-hydroxyphenyl residue was elucidated from the double intensity of the methine signals 27-H and 28-H, the HMBC correlations, and the ^{13}C chemical shifts, especially of C29 ($\delta_C = 156.2$ ppm). The phenolic proton gives rise to a singlet at $\delta_H = 9.33$ ppm, whose position was assigned from the nuclear Overhauser effect (NOE) with 28-H in the ROESY and NOESY spectra.

The HMBC spectrum also reveals that the quaternary carbon C22 ($\delta_C = 37.2$ ppm) correlates with a pair of geminal methyl groups C34/C35 ($\delta_H = 1.21$ and 0.92 ppm), and that the tertiary carbon atom C20 ($\delta_C = 74.3$ ppm) is connected to the remaining methyl group C33 ($\delta_H = 1.03$ ppm) and the hydroxy group 20-OH ($\delta_H = 4.48$ ppm) (Figure 1). Both quaternary carbons and their methyl substituents are adjacent to the methylene group C21 ($\delta_C = 59.7$ ppm) as judged by their HMBC correlations with the pair of geminal protons 21-Ha and 21-Hb ($\delta_H = 1.69$ and 1.55 ppm). Additional HMBC correlations observed for C23 and C19 allow the connection of the remaining bonds to give the tetrahydroindane core of elansolid A1 (**1**). The configuration of the double bonds of the *Z*,*E*,*Z*-triene in **1** was deduced from vicinal coupling constants and supported by appropriate ROESY data, while the *E* configuration at the $\Delta^{[4,5]}$ bond was determined from the ROESY correlations of 3-H, 5-H, and the methyl group C30.

Within the tetrahydroindane system the vicinal coupling constants acquired in [D$_6$]DMSO at 60 °C unambiguously indicate the *trans* configuration for 19-H, 23-H, and 24-H (J = 11.3–12 Hz) and a *gauche* orientation of 24-H and 16-H (J = 3.8 Hz). These findings were supported by NOEs between 24-H and 19-H and 16-H (Figure 2, left). Further ROESY

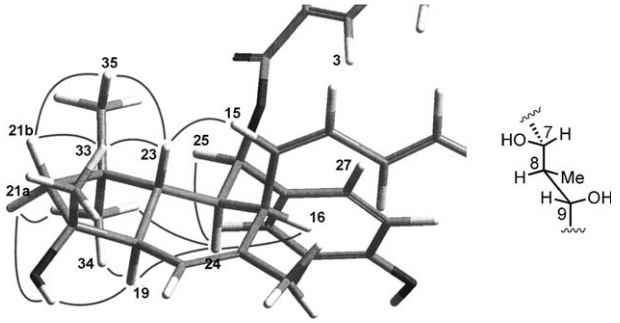

Figure 2. Partial view of a model of elansolid A1 (1) with selected nuclear Overhauser effects (left) and proposed stereogenic centers at C7–C9 in the lactone ring of 1 (right) with the relative stereochemistry R*. C gray, H white, O black.

correlations allowed identification of the relative positions of the substituents in the cyclopentane moiety: 1) 23-H shows NOEs with methyl groups C35 and C33 and both have NOEs with 21-Hb; 2) on the reverse face 19-H shows NOEs with 20-OH and the methyl group C34, while both have NOEs with 21-Ha. The strongest NOE was observed between 23-H and 15-H.

Additionally, the position of the lactone proton 25-H was determined from the observation of NOEs owing to the close proximity of both methyl groups C34 and C35. On the reverse face, the indistinguishable pair of aromatic protons 27-H show NOEs with 24-H, 16-H, and 3-H as well as the expected NOEs with 25-H and 28-H. Consequently, the lactone must be located at C25 as shown in Figure 2. The dihedral angle $\phi_{24H,25H}$ of 87° is in good agreement with the small vicinal coupling constant $^3J_{24,25}$ of 2.7 Hz. Thus, according to the NMR evidence, the relative stereochemistry of the core of elansolid A1 (**1**) is 16*R**,19*R**,20*R**,23*R**,24*R**,25*R**.[9]

Since the triene unit between C16 and C9 is expected to have a nearly planar conformation, the relative stereochemistry of the tetrahydroindane core of **1** can be extended from C16 to C9 in the second stereodomain: the coupling constant $^3J_{9,10}$ of 8.8 Hz indicates a *transoid* arrangement of protons 9-H and 10-H, which is supported by a very strong NOE between 9-H and 12-H. As the tetrahydroindane–triene and the diene–lactone are rigid moieties, the entire lactone ring must be highly strained, leaving no vacant inner space for either the 9-OH or the methyl group. Consequently, the 9-OH group should be *exo* oriented. Based on these considerations we conclude that the relative configuration at C9 is also *R**. A small coupling constant of about 4 Hz for $^3J_{8,9}$ and a large coupling constant of 8 Hz for $^3J_{7,8}$ (Table S1) indicate *gauche* and nearly staggered relative orientations (Figure 2, right), respectively, which also suggests *R** configurations of the stereogenic centers C7 and C8.

The complete assignment of the relative and absolute configurations of **1** was based on the seco acid derivatives **2** and **3** isolated from fermentation extracts (Scheme 1).

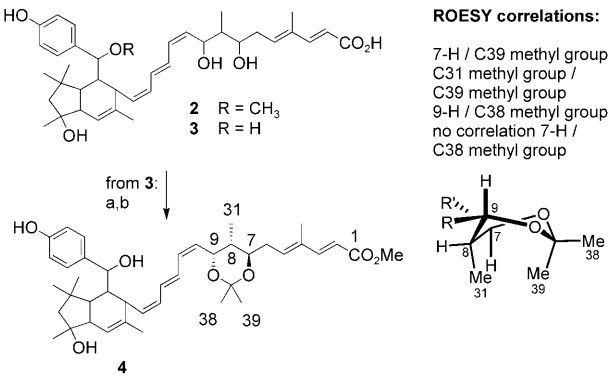

Scheme 1. Preparation of acetonide **4** and selected ROESY correlations.: a) CH_2N_2, EtOAc, RT, 71%; b) dimethoxypropane, PPTS, 18%. PPTS = pyridinium *p*-toluenesulfonate.

Derivative **2** may be an artifact resulting from a reaction with methanol during workup. As judged by HPLC/HR-ESI-MS elansolid B2 (**2**) has the elemental composition of **1** plus CH_3OH, that is, $C_{38}H_{52}O_7$. Compared to the NMR data of elansolid **1** the ^1H NMR spectrum of **2** in [D$_6$]acetone (Table S2) reveals an additional methoxy group at δ = 3.1 ppm and the 25-H doublet is shifted upfield by 1.3 ppm to $\delta = 4.64$ ppm. However, the doublet still shows the small vicinal coupling $J_{24,25}$ of 2.6 Hz, which is diagnostic for the 25*R** configuration of elansolid A1 (**1**) (Table S5).

The connection between the methoxy group and C25 was assigned from the NOE correlation with 25-H. Additional ROESY correlations supported the assigned 25*R** stereo-

chemistry, as the methoxy group shows correlations with 27-H and the methyl group C35. On the other hand, 25-H displays a strong ROESY correlation with the methyl group C34, while the aromatic protons 27-H show correlations with 16-H and 24-H.

Finally, we derivatized the 25-hydroxy variant elansolid B1 (**3**) (Scheme 1) which was also found in the crude extract of strain GBF13 and which was characterized in a similar manner to that described for B2 (**2**). The spectroscopically derived relationship between the stereocenters at C7, C8, and C9 (see above) was chemically determined by applying Rychnovsky's acetonide method as shown in Scheme 1.[10] The ^{13}C NMR spectrum of acetonide **4** shows characteristic shifts for the acetonide methyl groups at $\delta_C =$ 26.1 and 25.0 ppm and for the quarternary acetonide carbon at $\delta_C = 101.0$ ppm. These data suggest a 1,3-*trans* relationship of the stereocenters at C7 and C9 (see Figure 2, right). Since the dioxolane ring in **4** adopts a flexible twist conformation, unequivocal interpretation of the ROESY experiments is not possible. However, the observed correlations, for example between the C39 methyl group and 7-H, the C39 and the C31 methyl groups, and the C38 methyl group and 9-H, fully concur with the relative *R** stereochemistry of C7–C9. With this analysis in hand we initiated a synthetic program for finally proving the relative as well as the absolute stereochemistry at C7–C9 of **1**. For that purpose, elansolid B2 (**2**) was fragmented by treatment with ethylene in the presence of the second-generation Grubbs–Hoveyda catalyst to yield the two metathesis fragments **5** and **6**.

As outlined in Scheme 2 the total synthesis of enantiomerically enriched carboxylic acid **6** was achieved, and the product was compared with the fragment **6** obtained from the natural product. As the absolute configuration was unknown at this stage of the project, we arbitrarily decided to prepare the all-*R* isomer. The synthesis of **6** commenced with an *anti*-selective Masamune aldol reaction between the chiral ester **7** and the known aldehyde **8**[11] to yield the 2,3-*anti* product **9**.[12] After protection of the hydroxy group and cleavage of the auxiliary, the primary alcohol was oxidized to the corresponding aldehyde. This was alkylated using vinylmagnesium bromide to afford the allylic alcohols **10** and **11** in a diastereomeric ratio of 2:1. The relationship between the new hydroxy group at C5 and the fixed stereogenic center at C3 was assigned after formation of acetonides **12** and **13**, respectively, and their analysis using Rychnovsky's method. Functional-group manipulation and two successive Wittig reactions resulted in the complete assembly of the carbon skeleton. Finally, removal of all protecting groups and saponification of the ethyl ester in one step yielded the C1–C11 fragment **6** of the elansolids. Comparison of the optical rotations of the authentic sample obtained from elansolid B2 (**2**) {$[\alpha]_D^{20} = +32.5$ ($c = 0.12$, MeOH)} with the synthetic sample **6** {$[\alpha]_D^{20} = +24.8$ ($c = 0.40$, MeOH)} as well as their identical NMR spectra established simultaneously the relative and the absolute all-*R* configuration of the three stereogenic centers C7–C9. Since the relative configuration of elansolid A1 (**1**) had already been determined (see above), these results also established the six remaining stereogenic centers around the tetrahydroindane moiety and at C25 (Figure 3).

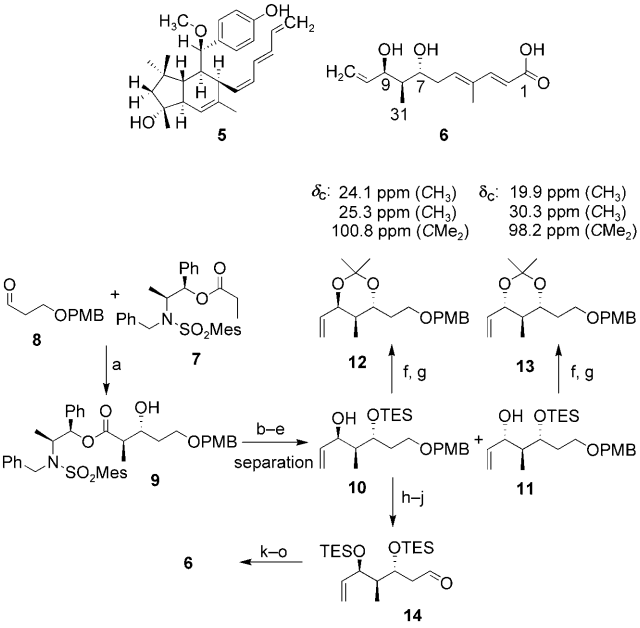

Scheme 2. Preparation of the eastern fragment **6**. Reagents and conditions: a) Et_3N, $(cy)_2BOTf$, CH_2Cl_2, −78 °C to 0 °C, 18 h, 79%; b) TESOTf, 2,6-lutidine, −78 °C, 70 min, 78%; c) DIBAL-H, CH_2Cl_2, −78 °C to −50 °C, 6 h, 81%; d) Dess–Martin periodinane, CH_2Cl_2, $NaHCO_3$, RT, 1.5 h; e) vinylmagnesium bromide, THF, −78 °C, 1.5 h, (4,5-*anti*/4,5-*syn* = 2:1), 78% for 2 steps; f) TBAF·3 H_2O, THF, 0 °C, 1 h, 86% for 4,5-*anti*, 84% for 4,5-*syn*; g) 2,2-dimethoxypropane, PPTS, CH_2Cl_2, RT, 1 h, 83% for 4,5-*anti* and for 84% 4,5-*syn*); h) TESOTf, 2,6-lutidine, CH_2Cl_2, −78 °C, 40 min, 81%; i) DDQ, CH_2Cl_2/buffer (pH 7), 0 °C, 2.5 h, 74%; j) Dess–Martin periodinane, CH_2Cl_2, $NaHCO_3$, RT, 18 h; k) (carbethoxyethylidene)triphenylphosphorane, $CHCl_3$, RT, 18 h, 74% for 2 steps; l) DIBAL-H, CH_2Cl_2, −78 °C, 1 h, 83%; m) Dess–Martin periodinane, CH_2Cl_2, $NaHCO_3$, RT, 18 h; n) (carbethoxymethylene)triphenylphosphorane, toluene, 60 °C, 5 d, 57% for 2 steps; o) 1 M LiOH, THF, MeOH, RT, 22 h, 54%. Cy = cyclohexyl, DDQ = 2,3-dichloro-5,6-dicyano-1,4-benzoquinone, DIBAL-H = diisobutylaluminum hydride, Mes = 2,4,6-trimethylphenyl, PMB = *para*-methoxybenzyl, TBAF = tetrabutylammonium fluoride, TES = triethylsilyl, Tf = trifluoromethansulfonyl.

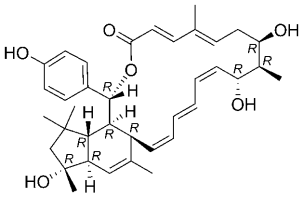

Figure 3. Absolute configuration of elansolid A1 (1).

In the course of a supplementary production of **1** an additional compound **1*** was identified in the analytical HPLC of the culture extract at 7.6 min with UV and MS data similar to that of elansolid A1 (**1**). Elansolid A2 (**1***) was isolated by preparative reversed-phase (RP) HPLC. Analysis of the NMR data in [D_6]DMSO at room temperature and at 70 °C (Table S4) unexpectedly resulted in the same structural formula. HPLC analyses revealed a slow interconversion of **1*** into **1** ([D_6]DMSO, RT, 55%, 6 d) while their chemical ring-opening lead to the same product, elansolid B (**2**)

[MeOH/H_2O (8:2), 0.1M NaOH 1%, RT]. We thus concluded that both compounds most likely represent atropisomers.

To unravel the conformational details of the atropisomers, their NMR data were compared more closely and molecular modeling was carried out. As several signals of interest of both elansolids are very broad in [D_6]DMSO, NMR spectra of **1** and **1*** were measured in [D_6]acetone (Table S5) at room temperature as well as at 250 K.

Molecular modeling started from the absolute all-*R* configuration of elansolid A1 (**1**). The dihedral angles from 5-H to 10-H were varied without any constraints using the "Conformational Search" module and finally the semiempirical PM3 method in HyperChem Version 8.5.[13] Solvent effects were not calculated, because the conformations are "frozen" by the ring strain and the stereochemistry of the four stereogenic centers in the lactone ring. The two structures representing the lowest local minima (Figure 4)[14] showed the expected high degree of similarity of their common structural units, that is, the tetrahydroindane system, the diene lactone unit, the triene unit, and the positions of the C8 and C9 substituents.

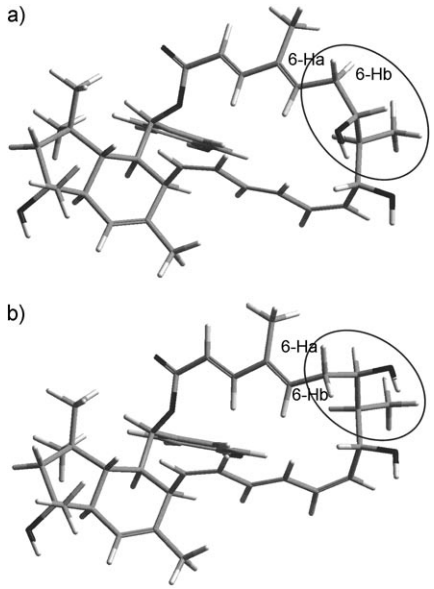

Figure 4. a) Model of elansolid A1 (1); b) model of elansolid A2 (1*). C gray, H white, to the pyrrole groups O black.

The NMR chemical shifts (δ) within the bicyclic tetrahydroindane core and the diene lactone unit of elansolids **1** and **1*** are nearly identical, and differences in chemical shifts but still identical coupling constants are observed within the triene unit. The major difference between the conformation-related NMR data of **1** and **1*** and between the two models are apparent in the lactone ring segment between methylene C6 and methine C8. While the model in Figure 4a shows a staggered arrangement of 7-H and 8-H ($\phi_{7H,8H} = 149°$) which corresponds well with the coupling $J_{7,8}$ of 9.4 Hz observed for elansolid A1 (**1**) (Table S8a), the model in Figure 4b, featuring a torsion angle $\phi_{7H,8H}$ of 61°, is compatible only with the coupling $J_{7,8}$ of 4.1 Hz of elansolid A2 (**1***) (Table S8b). The coupling constants between 5-H, 6-Ha/b, and 7-H also support this analysis.

Similarly, vicinal coupling constants for dihedral angles of the models were compared with the observed values (Tables S7a and S7b).[15] Both models account for the small vicinal coupling constants of 2–4 Hz observed between 8-H and 9-H in **1** and **1*** with dihedral angles of 78° and 71°, respectively. The relative position of the aromatic and the lactone rings at the tetrahydroindane moiety is also found to be similar in **1** and **1***, as another conspicuous small vicinal coupling constant of 1–3 Hz between 24H and 25H is consistent with dihedral angles of 87° and 77°, respectively.

The main conformational consequences of this atropisomerism are circled in Figure 4. In elansolid A1 (**1**) the methylene protons at C6 are directed to the outside of the lactone ring and the secondary alcohol C7 is "folded in" the lactone ring. This situation is reversed in elansolid A2 (**1***), where the model shows the methylene group C6 "folded in" while the hydroxy group at C7 is directed outwards. Consequently, the 7-OH and 9-OH groups assume a *cisoidal* relation in **1***, while a nearly orthogonal relation of the hydroxy groups is fixed in **1**, where 7-OH is directed to the front of the figure.

The intensities of ROESY correlations for selected atom distances in the atropisomers were also calculated and compared with the observed intensities (Tables S8a and S8b).[16] The three most intense nuclear Overhauser effects of the two elansolids were accounted for by atom distances between 1.8 and 1.9 Å for the proton pairs H-15/H-23, H-9/H-12, and H-13/H-16. Further comparison of selected distances and NOEs show a good agreement between the models and the ROESY NMR data. The anticipated ring strain stabilizing the isomers was indicated by diene and triene bonds deviating from planarity by 10.6° to 16.8° for dihedral angles $\phi_{1\text{-}O,2\text{-}H}$, $\phi_{11\text{-}H,12\text{-}H}$ und $\phi_{13\text{-}H,14\text{-}H}$ in the models of **1** and **1*** (Table S9, Figure 4).

The characteristic differences between conformations **1** and **1*** clearly rationalize the different physicochemical behavior, that is, retention times, which depend on the distribution of polarity on the surface of a molecule. Similarly, different biological effects, which are mainly controlled by hydrogen bonding between hydroxy groups of small molecules and their biological target, would be expected for the two stable conformational isomers. In fact, the two atropisomeric elansolids differ in their biological activity. While elansolid A2 (**1***) shows antibiotic activity against Gram-positive bacteria (Table S6) in the range between 0.2 and 64 $\mu g\,mL^{-1}$, elansolid A1 (**1**) is only weakly active. Similarly, no cytotoxicity was observed with L929 mouse fibroblast cells for atropisomer A1 (**1**) up to 40 $\mu g\,mL^{-1}$ while the conformer elansolid A2 (**1***) showed an IC_{50} value of 12 $\mu g\,mL^{-1}$.

Solvent-dependent equilibria of folded-in and folded-out conformations have been observed in, for example, the 14-membered macrolide antibiotics erythromycin and oleandromycin, and the 16-membered macrolide tylosin.[17] The elansolids A1 (**1**) and A2 (**1***) differ from these examples as the rigidity of their macrocyclic rings sustains the atropisomerism more firmly.[18] Similar to elansolids A1 (**1**) and A2 (**1***) atropisomerism of small rings lacking steric repulsion has

been observed, for example, in the case of abyssomycin C and its synthetic counterpart *atrop*-abyssomicin C.[19] Our future work is directed towards deciphering the biosynthesis of this structurally unique class of macrolactones.

Received: August 20, 2010
Published online: December 8, 2010

Keywords: antibiotics · atropisomers · *Chitinophaga* · molecular modeling · structure elucidation

[1] SQ 28332, 28502, 28503: a) R. Cooper, K. Bush, P. A. Principe, W. H. Trejo, J. S. Wels, R. B. Sykes, *J. Antibiot.* **1983**, *36*, 1252–1257; b) R. Cooper, *J. Antibiot.* **1983**, *36*, 125—1262; c) P. D. Singh, J. H. Johnson, P. C. Ward, J. S. Wells, W. H. Trejo, R. B. Sykes, *J. Antibiot.* **1983**, *36*, 1245–1251. FR901451: T. Fujita, H. Hatanaka, K. Hayashi, N. Shigematsu, S. Takase, M. Okamoto, M. Okuhara, K. Shimatani, A. Satoh, *J. Antibiot.* **1994**, *47*, 1359–1364. FR901451: T. Fujita, H. Hatanaka, K. Hayashi, N. Shigematsu, S. Takase, M. Okamoto, M. Okuhara, K. Shimatani, A. Satoh, *J. Antibiot.* **1994**, *47*, 1359–1364. YM-47141 and YM-47142: d) K. Yasumuro, Y. Suzuki, M. Shibazaki, K. Teramura, K. Abe, M. Orita, *J. Antibiot.* **1995**, *48*, 1425–1429; e) M. Orita, K. Yasumuro, K. Kokubo, M. Shimizu, K. Abe, T. Tokunaga, H. Kaniwa, *J. Antibiot.* **1995**, *48*, 1430–1434. Topostin: f) K. Suzuki, H. Yamaguchi, S. Miyazaki, K. Nagai, S.-I. Watanabe, T. Saito, K. Ishii, M. Hanada, T. Sekine, Y. Ikegami, T. Andoh, *J. Antibiot.* **1990**, *43*, 154–157; g) Y. Ikegami, N. Takeuchi, M. Hanada, Y. Hasegawa, K. Ishii, T. Andoh, T. Sato, K. Suzuki, H. Yamaguchi, S. Miyazaki, K. Nagai, S.-J. Watanabe, T. Saito, *J. Antibiot.* **1990**, *43*, 158–162.

[2] N. Katayama, Y. Nozaki, K. Okonogi, H. Ono, S. Harada, H. Okazaki, *J. Antibiot.* **1985**, *38*, 1117–1125; T. Hida, S. Tsubotani, N. Katayama, H. Okazaki, S. Harada, *J. Antibiot.* **1985**, *38*, 1128–1140.

[3] MRSA = methicillin-resistant *Staphylococcus aureus.*

[4] N. Katayama, S. Fukusumi, Y. Funabashi, T. Iwahi, H. J. Ono, *J. Antibiot.* **1993**, *46*, 606–613.

[5] N. Böddeker, G. Bahador, C. Gibbs, E. Mabery, J. Wolf, L. Xu, J. Watson, *RNA* **2002**, *8*, 1120–1128.

[6] G. Höfle, GBF-internal Annual Report, unpublished.

[7] P. Kämpfer, C. C. Young, K. R. Sridhar, A. B. Arun, W. A. Lai, F. T. Shen, P. D. Rekha, *Int. J. Syst. Evol. Microbiol.* **2006**, *56*, 2223–2228.

[8] K. Gerth, H. Steinmetz, G. Höfle, EP 2 093 212A1, **2009**.

[9] "*R**" denotes relative *R* stereochemistry.

[10] a) S. D. Rychnovsky, D. J. Skalitzky, *Tetrahedron Lett.* **1990**, *31*, 945–948; b) S. D. Rychnovsky, B. N. Rogers, T. I. Richardson, *Acc. Chem. Res.* **1998**, *31*, 9–17; c) D. A. Evans, D. L. Rieger, J. R. Gage, *Tetrahedron Lett.* **1990**, *49*, 7099–7100.

[11] F. M. Cordero, F. Pisaneschi, M. Gensini, A. Goti, A. Brandi, *Eur. J. Org. Chem.* **2002**, *12*, 1941–1951.

[12] T. Inoue, J. Liu, D. C. Buske, A. Abiko, *J. Org. Chem.* **2002**, *67*, 5250–5256; A. Abiko, J. Liu, S. Masamune, *J. Am. Chem. Soc.* **1997**, *119*, 2586–2587.

[13] The conformational search option in HyperChem aims to find the conformations that constitute local energy minima. It does so by randomly initializing torsional angles and performing subsequent MM+ optimizations, looking for unique conformations that are local energy minima.

[14] Calculated energies: (**1**): PM3: $E = -9368.31$ kcal mol^{-1}; MM+: 44.456 kcal mol^{-1}; (**1***): PM3: $E = -9370.85$ kcal mol^{-1}; MM+: 44.410 kcal mol^{-1}. Color figures are presented in the Supporting Information.

[15] C. A. G. Haasnoot, F. A. A. M. DeLeeuw, C. Altona, *Tetrahedron* **1980**, *36*, 2783–2792 (http://www.stenutz.eu/conf/haasnoot.php).

[16] D. A. Evans, M. J. Bodkin, S. R. Baker, G. J. Sharman, *Magn. Reson. Chem.* **2007**, *45*, 595–600 (Janocchio—a Java applet for viewing 3D structures and calculating NMR couplings and NOEs: http://janocchio.sourceforge.net/).

[17] a) W. E. Steinmetz, J. D. Sadowsky, J. S. Rice, J. J. Roberts, Y. K. Bui, *Magn. Reson. Chem.* **2001**, *39*, 163–172; b) P. Novak, Z. B. Tomisic, P. Tepes, G. Lazarevski, J. Plavec, G. Turkalj, *Org. Biomol. Chem.* **2005**, *3*, 39–47; c) P. M. Ivanov, *J. Mol. Struct.* **2002**, *606*, 217–229.

[18] G. Bringmann, A. J. Price Mortimer, P. A. Keller, M. J. Gresser, J. Garner, M. Breuning, *Angew. Chem.* **2005**, *117*, 5518–5563; *Angew. Chem. Int. Ed.* **2005**, *44*, 5384–5427.

[19] K. C. Nicolaou, S. T. Harrison, *J. Am. Chem. Soc.* **2007**, *129*, 429–440, and references therein.

